On the spatial and temporal shift in the archetypal seasonal temperature cycle as driven by annual and semi-annual harmonics

Joshua S. North, Erin M. Schliep, Christopher K. Wikle

Department of Statistics
University of Missouri

August 4, 2020

Overview

Understanding how spatial patterns in environmental seasonal cycles vary through time is needed to understand the symbiotic relationships.

- Native bark beetle infestations (Bentz et al., 2010).
- Ocean primary productivity (Defriez et al., 2016).
- Lake stratification (Kraemer et al., 2015).
- Migration patterns (Usui et al., 2017).

Overview

- The seasonal cycle in atmospheric variables is a direct response to the variation in solar insolation due to the Earth's orbital path around the Sun.
- The atmospheric response to the overhead sun crossing the equator twice a year suggests a more complicated seasonal variation that includes both an annual and a semi-annual harmonic.
- Harmonic analysis has been used to characterize the connection between these harmonics and the observed seasonal cycle.
- Restrict our estimation to the first two harmonics, and refer to a "cycle" as the sum of the first and second harmonics hereafter.

Data

- Air temperature (deg C) data at two meters above the surface obtained from the National Center for Environmental Prediction (NCEP) Reanalysis[1].
- The spatial domain of interest spanned the continental United States and portions of Mexico and Canada.
- We thinned the data spatially to reduce the overall dimension, keeping every other location in both the longitudinal and latitudinal directions.
- Daily minimum and maximum temperature values at 3621 spatial locations over 40 years, for a total of over 1.06×10^8 data points.
- All temperature time series were centered since the focus of inference is on the harmonics and change in harmonics as opposed to raw temperature.

[1] https://www.esrl.noaa.gov/psd/

Fourier Representation

Let z_t denote temperature on day t where $t = 1, \ldots, T$, and T is the number of days in the year. Expressing the time series as a Fourier series:

1. Amplitude-phase,

$$z_t = a_0 + \sum_{h=1}^{T/2} A_h \cos\left(\frac{2\pi ht}{T} + \varphi_h\right)$$

2. Sine-cosine form

$$z_t = a_0 + \sum_{h=1}^{T/2} \left[a_h \cos\left(\frac{2\pi th}{T}\right) + b_h \sin\left(\frac{2\pi th}{T}\right)\right]$$

A_h and φ_h are the amplitude and phase, respectively, and a_h and b_h are the Fourier coefficients for the h^{th} harmonic. The amplitude/phase and coefficients are related by $A_h = \sqrt{a_h^2 + b_h^2}$, $A_h \in [0, \infty)$, and $\varphi_h = \tan^{-1}(-b_h/a_h)$, $\varphi_h \in [-\pi/h, \pi/h]$.

Exploratory Data Analysis - Semi-Annual Importance

The semi-annual harmonic affects the seasonal cycle differently depending on spatial location and time.

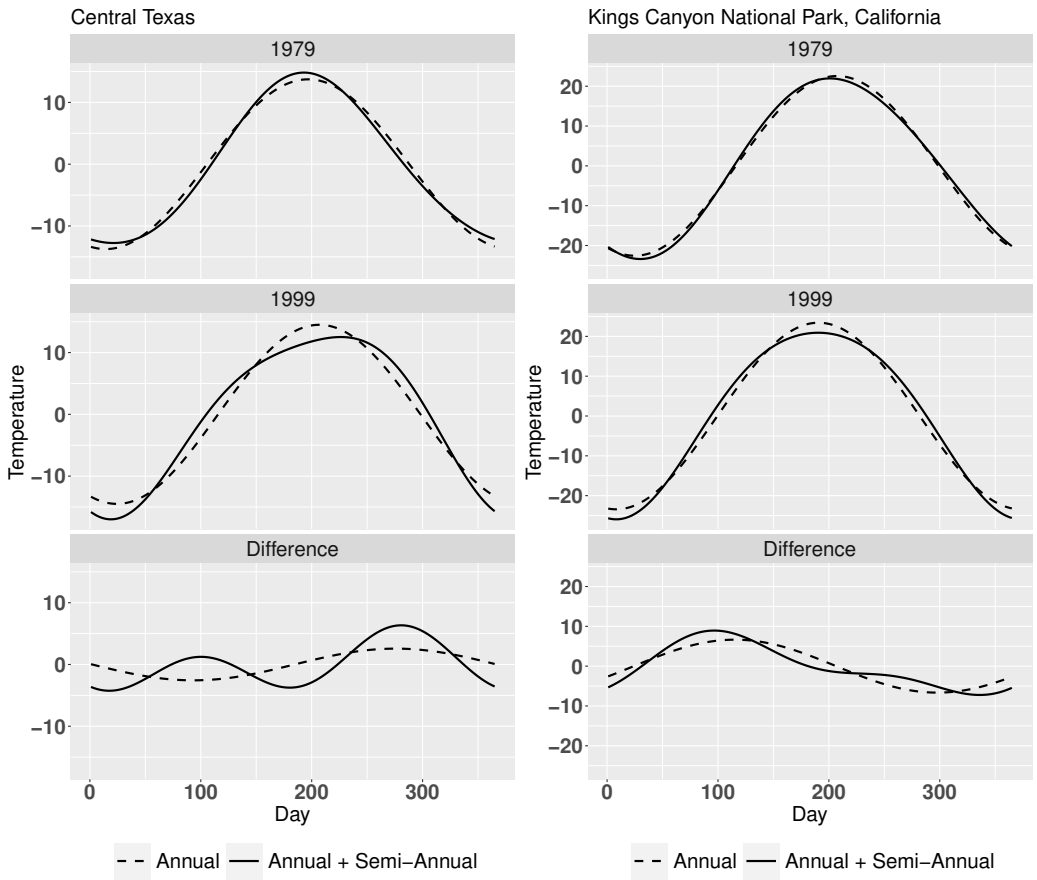

Exploratory Data Analysis - Minimum Temperature

Spatial patterns in the estimates.

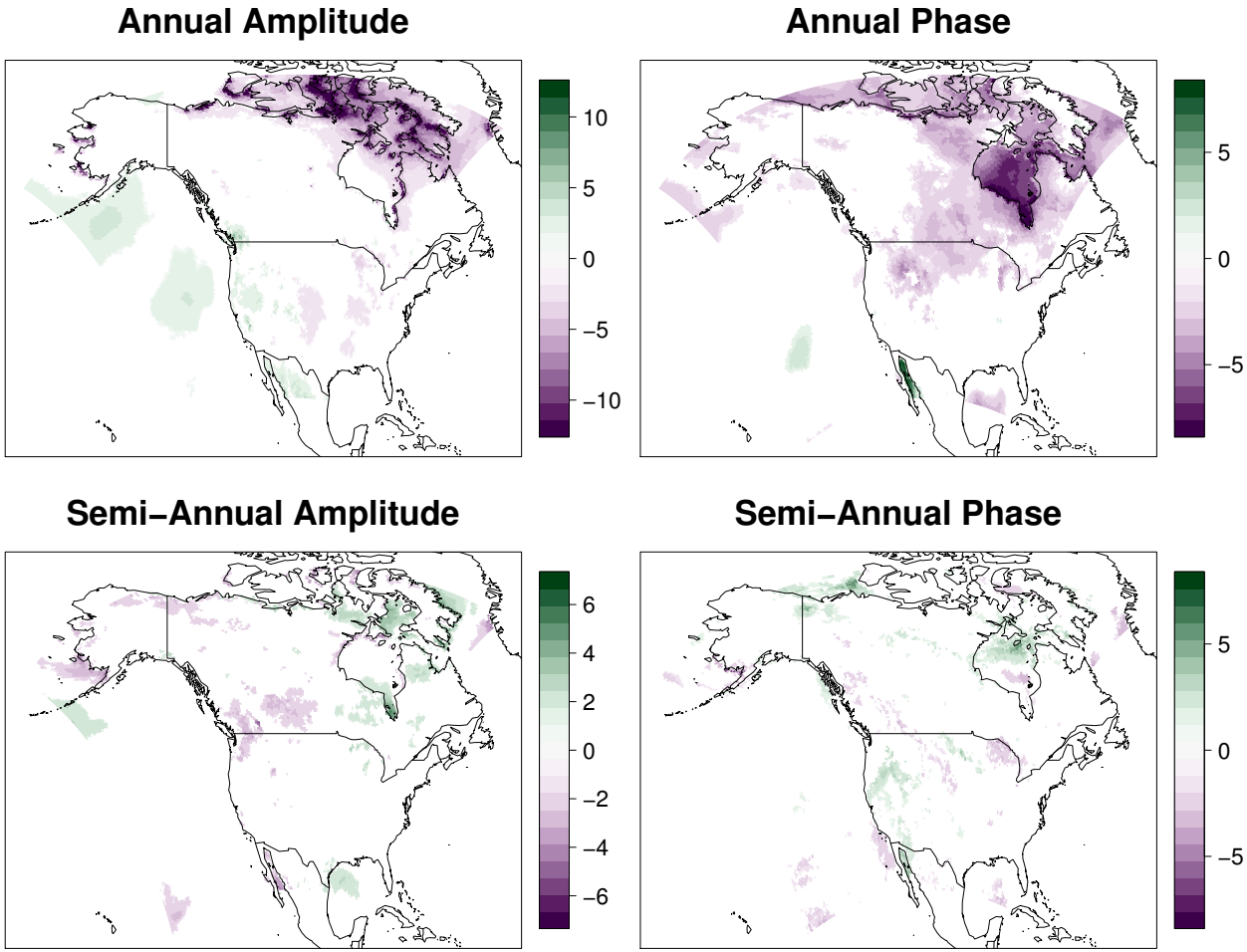

Exploratory Data Analysis - Maximum Temperature

Similarity to the minimum temperature estimates.

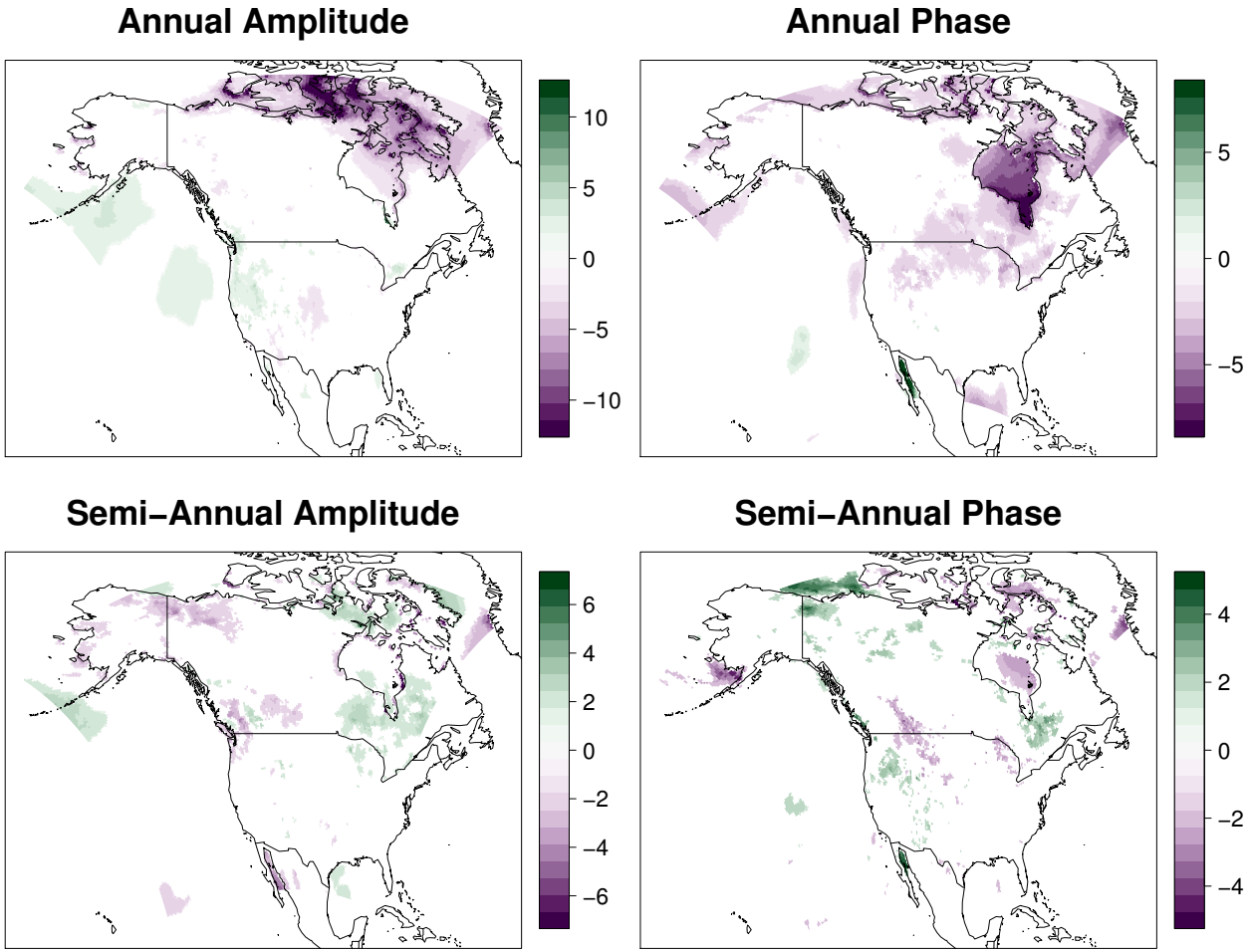

Model Goals

Goal: Quantify the spatial and temporal change in minimum and maximum temperature seasonal cycles as a function of the annual and semi-annual harmonics.

- Capture spatial dependence.
- Capture temporal dynamics.
- Capture multivariate dependence of these harmonics through spatially and temporally-varying coefficients.

Data Model

Let $\boldsymbol{z}_{1\ell}(\boldsymbol{s}) = [z_{11}(\boldsymbol{s}), ..., z_{1T_\ell}(\boldsymbol{s})]'$ and $\boldsymbol{z}_{2\ell}(\boldsymbol{s}) = [z_{21}(\boldsymbol{s}), ..., z_{2T_\ell}(\boldsymbol{s})]'$ denote minimum and maximum temperature, respectively, where T_ℓ is the number of days in year year $\ell = 1, ..., L$, at location $\boldsymbol{s} \in \{\boldsymbol{s}_1, ..., \boldsymbol{s}_n\}$. The linear model for temperature is

$$\boldsymbol{z}_{j\ell}(\boldsymbol{s}) = \boldsymbol{X}_\ell \widetilde{\boldsymbol{\beta}}_{j\ell}(\boldsymbol{s}) + \widetilde{\boldsymbol{\epsilon}}_{j\ell}(\boldsymbol{s}) \qquad j = 1, 2,$$

where

$$\boldsymbol{X}_\ell = \Big[\cos(2\pi(t-1)/T_\ell), \sin(2\pi(t-1)/T_\ell), \cos(4\pi(t-1)/T_\ell), \sin(4\pi(t-1)/T_\ell) \Big]_{t=1,...,T_\ell},$$

$\widetilde{\boldsymbol{\beta}}_{j\ell}(\boldsymbol{s}) = [a_1(\boldsymbol{s}), b_1(\boldsymbol{s}), a_2(\boldsymbol{s}), b_2(\boldsymbol{s})]'$, and $\widetilde{\boldsymbol{\epsilon}}_{j\ell}(\boldsymbol{s})$ are iid $\text{Gau}(0, \widetilde{\sigma}^2_{\varepsilon_j}(\boldsymbol{s})\, \boldsymbol{I}_{T_\ell})$.

Parameter Model

The spatially varying harmonic coefficients evolve according to a random walk:

$$\widetilde{\boldsymbol{\beta}}_\ell(\boldsymbol{s}) \mid \widetilde{\boldsymbol{\beta}}_{\ell-1}(\boldsymbol{s}), \widetilde{\boldsymbol{w}}_\ell(\boldsymbol{s}) \sim \text{Gau}\left(\widetilde{\boldsymbol{\beta}}_{\ell-1}(\boldsymbol{s}) + \widetilde{\boldsymbol{w}}_\ell(\boldsymbol{s}), \widetilde{\boldsymbol{\Sigma}}_\beta\right)$$

where $\widetilde{\boldsymbol{\beta}}_\ell(\boldsymbol{s}) = \left[\widetilde{\boldsymbol{\beta}}_{1\ell}(\boldsymbol{s})', \widetilde{\boldsymbol{\beta}}_{2\ell}(\boldsymbol{s})'\right]'$, $\widetilde{\boldsymbol{\Sigma}}_\beta$ is an 8×8 unstructured covariance matrix, $\widetilde{\boldsymbol{w}}_\ell(\boldsymbol{s}) = \left[\widetilde{\boldsymbol{w}}_{1\ell}(\boldsymbol{s})', \widetilde{\boldsymbol{w}}_{2\ell}(\boldsymbol{s})'\right]'$ with $\widetilde{\boldsymbol{w}}_{j\ell}(\boldsymbol{s}) = [\widetilde{w}_{j1\ell}(\boldsymbol{s}), ..., \widetilde{w}_{j4\ell}(\boldsymbol{s})]'$, and

$$\widetilde{w}_{jk\ell}(\boldsymbol{s}) \overset{\text{ind.}}{\sim} \textit{Gaussian Process}\left(0, C\left(\cdot; \boldsymbol{\theta}_{jk}\right)\right).$$

Parameter Model

- For the Gaussian Process, we assume an exponential covariance function, where $C(\boldsymbol{s}, \boldsymbol{s}'; \boldsymbol{\theta}_{jk}) = \sigma^2_{jk} \exp\{-||\boldsymbol{s} - \boldsymbol{s}'||/\phi_{jk}\}$, $||\boldsymbol{s} - \boldsymbol{s}'||$ is the Euclidean distance between locations $\boldsymbol{s}$ and $\boldsymbol{s}'$, and $\boldsymbol{\theta}_{jk} = \{\sigma^2_{jk}, \phi_{jk}\}$ consists of the spatial variance and decay parameters, respectively, for process $k = 1, ..., p$.

- $\widetilde{\boldsymbol{w}}_\ell(\boldsymbol{s})$ accounts for the residual spatial variation in the Fourier coefficients between year $\ell - 1$ and ℓ.

Spatial Structure - Computational Bottleneck

- Model inference presents computational challenges due to the number of spatial locations, years, harmonics, and processes.
- A single draw from the conditional distribution of $\widetilde{\boldsymbol{\beta}}_\ell \mid \widetilde{\boldsymbol{\beta}}_{\ell-1}, \widetilde{\boldsymbol{w}}_\ell$ requires matrix operations on an $8n \times 8n$ matrix (i.e. $\approx 29,000 \times 29,000$).
- We use spatio-temporal predictive processes (Finley et al., 2012) to enhance computational efficiency.

Spatial Structure - Predictive Process

- $\mathbb{S} = \{\boldsymbol{s}_1, ..., \boldsymbol{s}_n\}$ are the locations where data are available.
- $\mathbb{S}^* = \{\boldsymbol{s}_1^*, ..., \boldsymbol{s}_m^*\}$ knot locations where $m \ll n$.
- The predictive process is $w_{jk\ell}(\boldsymbol{s}) = E(\widetilde{w}_{jk\ell}(\boldsymbol{s})|\widetilde{\boldsymbol{w}}^*_{jk\ell}) = \boldsymbol{c}(\boldsymbol{s};\boldsymbol{\theta}_{jk})'\boldsymbol{C}^*(\boldsymbol{\theta}_{jk})^{-1}\widetilde{\boldsymbol{w}}^*_{jk\ell}$, where $\widetilde{\boldsymbol{w}}^*_{jk\ell} = [\widetilde{w}_{jk\ell}(\boldsymbol{s}_1^*), ..., \widetilde{w}_{jk\ell}(\boldsymbol{s}_m^*)]'$.
- $\boldsymbol{c}(\boldsymbol{s};\boldsymbol{\theta}_{jk})' = [C(\boldsymbol{s}, *;\boldsymbol{\theta}_{jk})]_{1\times m}$ and $\boldsymbol{C}^*(\boldsymbol{\theta}_{jk}) = [C(*, *;\theta_{jk})]_{m\times m}$.

Final Model

The resulting distribution of the coefficients is

$$\boldsymbol{\beta}_\ell(\boldsymbol{s}) \mid \boldsymbol{\beta}_{\ell-1}(\boldsymbol{s}), \boldsymbol{w}_\ell(\boldsymbol{s}) \sim \text{Gau}\left(\boldsymbol{\beta}_{\ell-1}(\boldsymbol{s}) + \boldsymbol{w}_\ell(\boldsymbol{s}), \boldsymbol{\Sigma}_\beta\right),$$

and the data model can be rewritten in the form of the predictive process,

$$\boldsymbol{z}_{j\ell}(\boldsymbol{s}) \mid \boldsymbol{\beta}_{j\ell}(\boldsymbol{s}) \sim \mathit{Gau}(\boldsymbol{X}_\ell \boldsymbol{\beta}_{j\ell}(\boldsymbol{s}), \sigma^2_{\varepsilon_j}(\boldsymbol{s})\, \boldsymbol{I}_{T_\ell}), \qquad j = 1, 2.$$

Therefore, conditioned on the predictive process, the coefficient process is spatially independent.

Hyperparameter Specification

- For $\sigma^2_{\epsilon_\ell}(\boldsymbol{s})$, the variance for location $\boldsymbol{s}$ that is shared across time is modeled $\sigma^2_{\epsilon_j}(\boldsymbol{s}) \sim$ Inv-Gamma(a, b).
- For the 8×8 covariance matrix of the β parameters we assign $\boldsymbol{\Sigma}_\beta \sim$ Inv-Wishart$(\boldsymbol{V}, \xi)$.
- For the spatial variance for the k^{th} spatial process is modeled $\sigma^2_{jk} \sim$ Inv-Gamma(a_{jk}, b_{jk}).
- All hyperpriors were chosen such that the priors have finite first moments.
- Preliminary analyses with a uniform prior distribution for ϕ_{jk} indicated that this parameter had little impact on the inference of the parameters of interest $(\phi_{jk} = \phi)$.
- For the predictive process, 144 knot locations evenly spaced across the domain of interest.

Model Inference

- To improve computational efficiency of our sampling algorithm, we took advantage of parallel computation when possible (i.e., $\boldsymbol{\beta}_\ell | \boldsymbol{w}_\ell$ are spatially independent).
- Posterior inference will focus on the comparison of the amplitude and phase of the annual and semi-annual harmonics across all years and spatial locations.
- Important characteristics of these cycles, such as the day at which the cycle reached its peak or trough, can also be computed.
  - Peak and trough days can be compared across time to quantify shifts in temperature cycles.

Results

Shift in the peak day of the minimum and maximum temperature cycles.

Peak Day Maximum Temperature

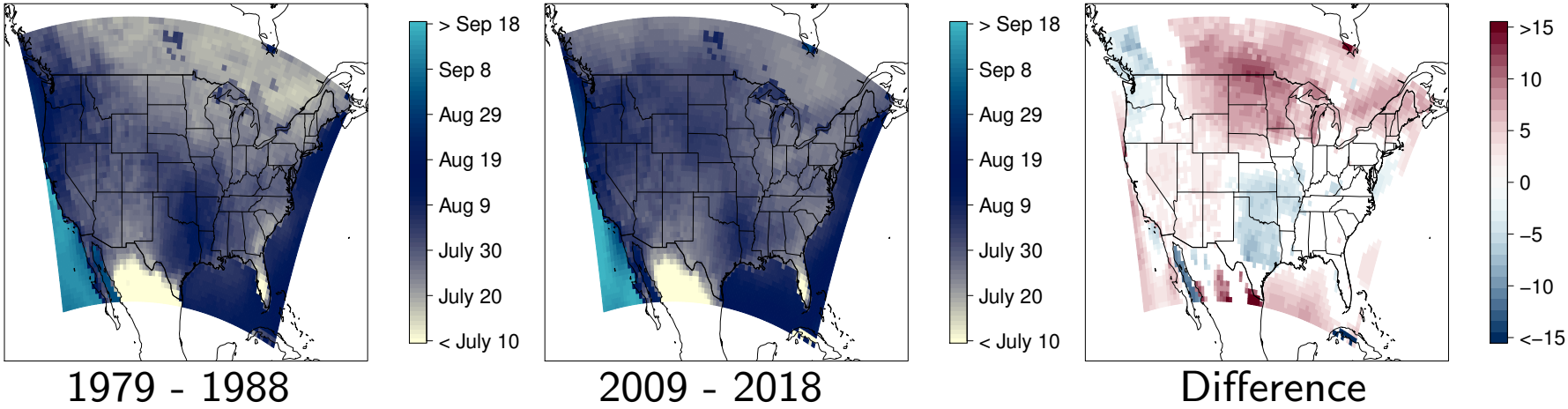

Peak Day Minimum Temperature

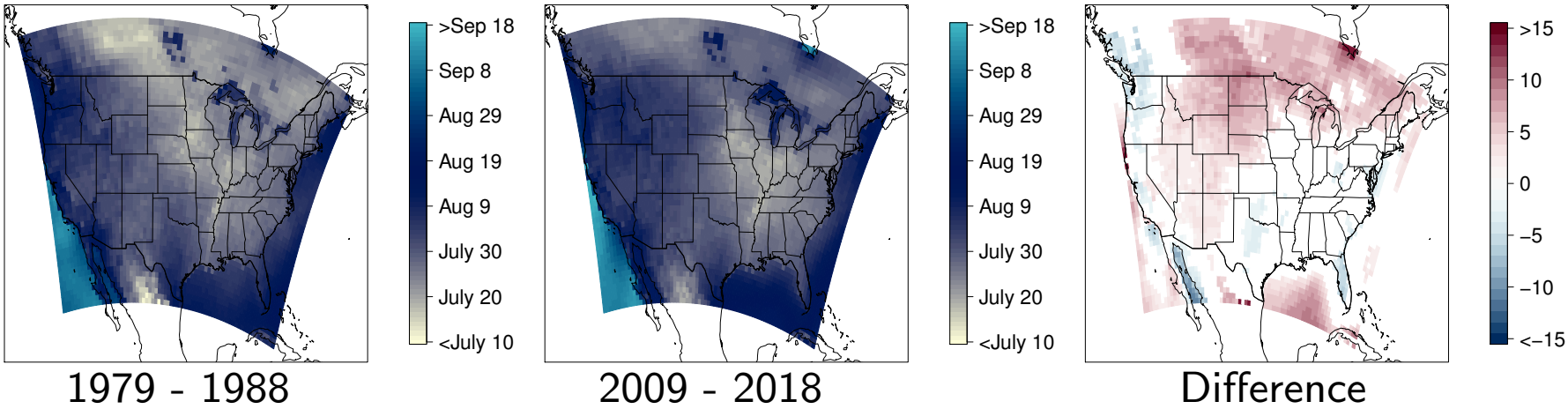

Results

Shift in the trough day of the minimum and maximum temperature cycles.

Trough Day Maximum Temperature

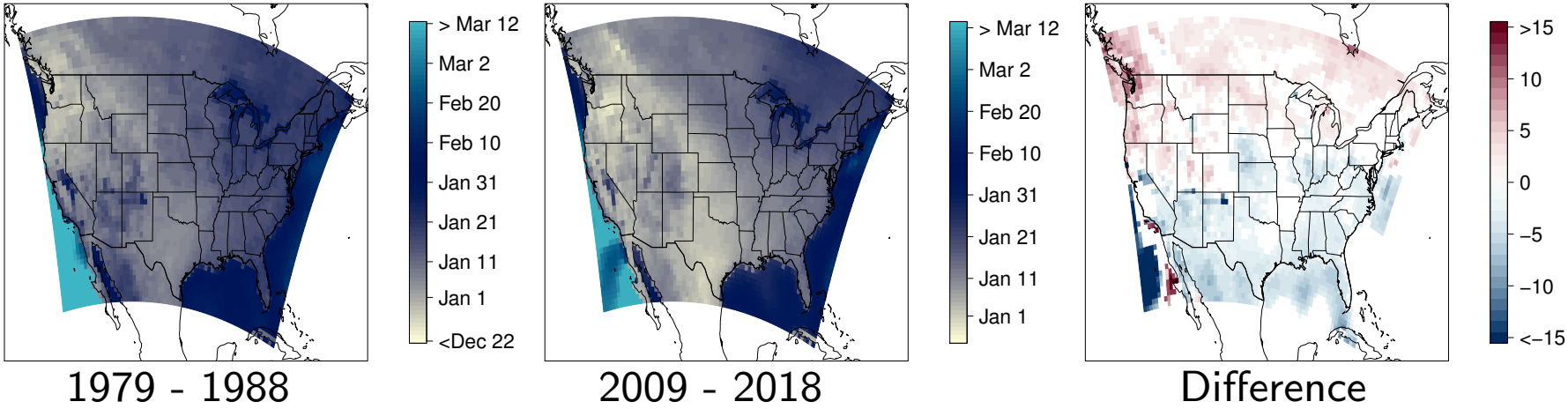

1979 - 1988 | 2009 - 2018 | Difference

Trough Day Minimum Temperature

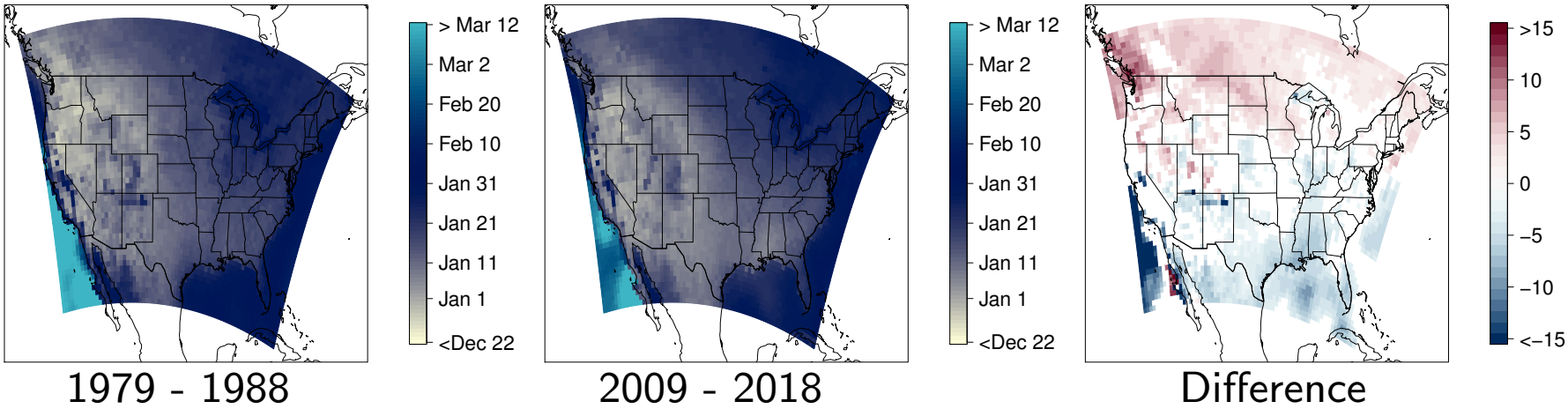

1979 - 1988 | 2009 - 2018 | Difference

Semi-Annual Importance

Effect of including semi-annual harmonic.

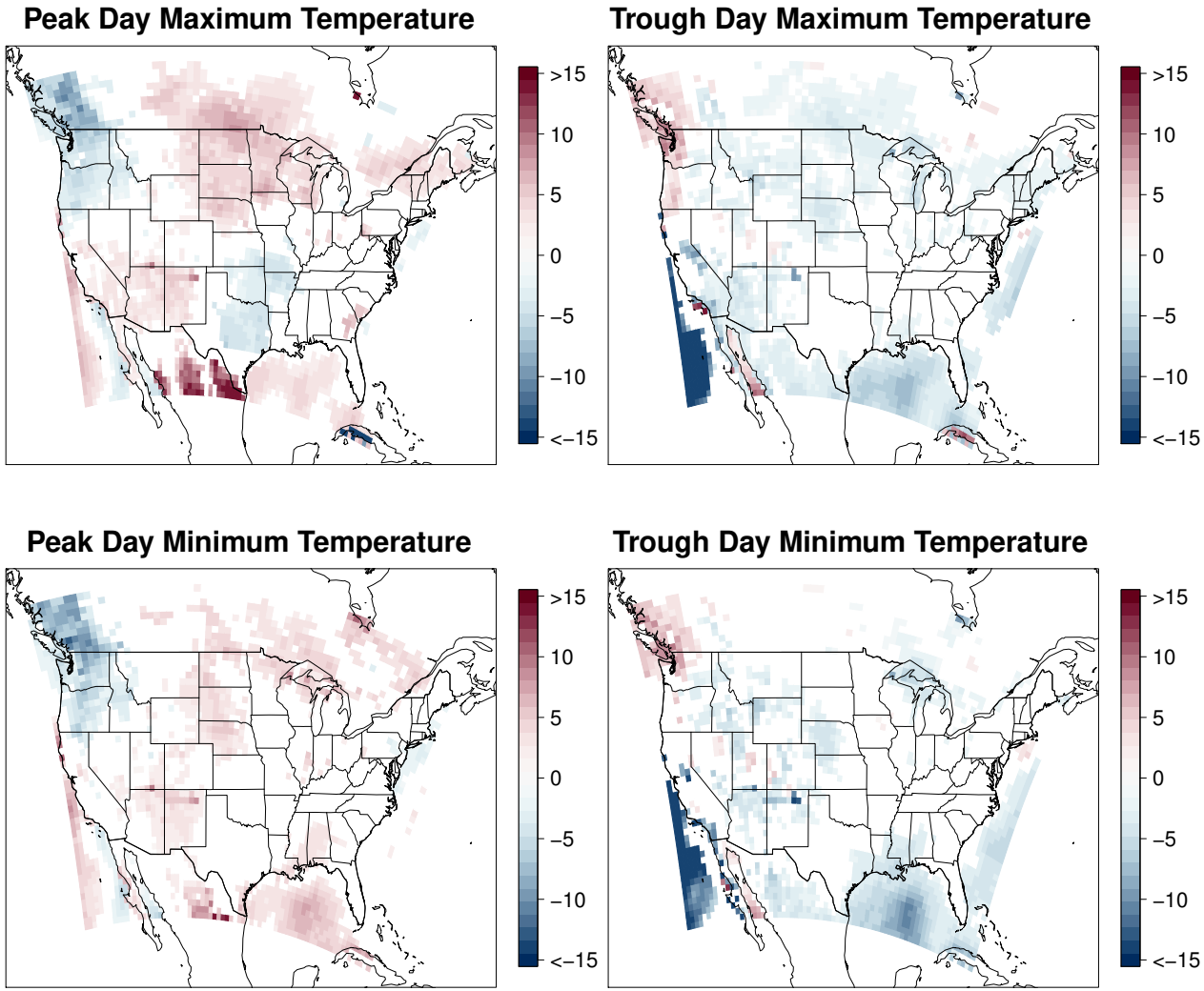

Conclusion

- Modeled the spatial and temporal change in minimum and maximum temperature seasonal cycles as a function of the annual and semi-annual harmonics.
- Used the predictive process for spatial dimension reduction.
- Obtained inference on the amplitude and phase of the annual and semi-annual harmonics.
- Highlighted areas where the seasonal temperature cycle has changed.
- Highlighted the importance of including the semi-annual harmonic when investigating the change in seasonal cycle.

Thank You!

Joshua North
joshuanorth@mail.missouri.edu

References I

Bentz, B. J., Régnière, J., Fettig, C. J., Hansen, E. M., Hayes, J. L., Hicke, J. A., Kelsey, R. G., Negrón, J. F., and Seybold, S. J. (2010). Climate Change and Bark Beetles of the Western United States and Canada: Direct and Indirect Effects. *BioScience*, 60(8):602–613. doi:10.1525/bio.2010.60.8.6.

Defriez, E. J., Sheppard, L. W., Reid, P. C., and Reuman, D. C. (2016). Climate change-related regime shifts have altered spatial synchrony of plankton dynamics in the North Sea. *Global Change Biology*, 22(6):2069–2080. doi:10.1111/gcb.13229.

Finley, A. O., Banerjee, S., and Gelfand, A. E. (2012). Bayesian dynamic modeling for large space-time datasets using Gaussian predictive processes. *Journal of Geographical Systems*, 14(1):29–47. doi:10.1007/s10109-011-0154-8.

Kraemer, B. M., Anneville, O., Chandra, S., Dix, M., Kuusisto, E., Livingstone, D. M., Rimmer, A., Schladow, S. G., Silow, E., Sitoki, L. M., Tamatamah, R., Vadeboncoeur, Y., and McIntyre, P. B. (2015). Morphometry and average temperature affect lake stratification responses to climate change. *Geophysical Research Letters*, 42(12):4981–4988. doi:10.1002/2015GL064097.

Usui, T., Butchart, S. H. M., and Phillimore, A. B. (2017). Temporal shifts and temperature sensitivity of avian spring migratory phenology: a phylogenetic meta-analysis. *Journal of Animal Ecology*, 86(2):250–261. doi:10.1111/1365-2656.12612.